Silver Jubilee for the OSIRIS spectrometer: Achievements and Outlook

Franz Demmel[1,*], *Adrien* Perrichon[1], *David* McPhail[1], *Paula* Luna Dapica[1], *Nick* Webb[1], *Andy* Cook[1], *Erik* Schooneveld[1], *Johnny* Boxall[1], *Nigel* Rhodes[1], *Cyril* Lockett[2], *Colin* Dabinett[2], *Joel* Hodder[2], *Daniel* Nye[1], *Sanghamitra* Mukhopadhyay[1], *Ian* Silverwood[1], *Mona* Sarter[1], *Victoria* Garcia Sakai[1], and *Felix* Fernandez-Alonso[3,4,5]

[1]ISIS Facility, STFC, Didcot, OX11 0QX, United Kingdom
[2]Technology Department, STFC, Didcot, OX11 0QX, United Kingdom
[3]Materials Physics Center, CSIC-UPV/EHU, Paseo Manuel de Lardizabal 5, 20018 Donostia - San Sebastian, Spain
[4]Donostia International Physics Center (DIPC), Paseo Manuel de Lardizabal 4, 20018 Donostia - San Sebastian, Spain
[5]IKERBASQUE, Basque Foundation for Science, Plaza Euskadi 5, 48009 Bilbao, Spain

Abstract. In December 1997 the Osiris beamline at the ISIS facility, UK, recorded its first neutron spectrum. The instrument enjoyed a first stint as a cold neutron diffractometer before the spectroscopic capabilities were fully commissioned. Osiris soon became a workhorse quasielastic spectrometer as well as a highly successful low-energy spectrometer. The status of the instrument is recognized by the user community with high-impact publications ranging from energy materials over life science to quantum matter. To enhance the existing capabilities a silicon analyzer is under construction. The primary spectrometer will be upgraded with a new supermirror guide providing a factor 10 to 14 increased flux in combination with a new hydrogen moderator. Beyond these developments further improvements of the energy resolution with a combination of a fast pulse shaping chopper and using a direct backscattering geometry are being investigated.

1 Introduction

The Osiris instrument at the ISIS facility recorded its first spectrum in December 1997. At that time it went into operation as a cold neutron diffractometer and a few years later the spectrometer capabilities were installed and commissioned [1–7]. This indirect spectrometer is based on the concept of analyzing the incoming energy through the time-of-flight (tof) and the fixed final energy through Bragg scattering from a near-backscattering crystal analyzer. Further improvements were made with the installation of a movable Beryllium filter to remove the higher order reflections of the pyrolytic graphite analyzer [8].

The strength of this spectrometer concept lies in the combination of a relative high energy resolution due to the near-backscattering geometry (FWHM = 25 μeV for the PG002 reflection) over a wide range of momentum transfers with a large dynamic range (up to several meV in energy transfer) due to the tof-technique. These characteristics allowed successful experiments in the field of high resolution low-energy spectroscopy. The spin dynamics of strongly correlated electrons materials was unraveled, which often required single crystal experiments with high magnetic fields in combination with dilution fridge temperatures [9–12]. Materials for energy research had a prominent role in the research programme of Osiris from the beginning [13]. The high sensitivity of the spectrometer, which reaches a factor 10000 in signal to background [6], benefitted QENS-studies on ion mobility. Novel elec-

trode materials for batteries [14, 15] have been investigated, the mobility of protons and hydride ions was studied [16, 17] and details about materials for future photovoltaic applications could be revealed [18]. More recently the quasielastic response to pressure of barocaloric materials was resolved [19]. QENS was also applied studying the diffusion of small molecules in framework materials for catalytic applications and attracted a growing user community [20, 21]. Within softmatter and bioscience the relaxations and mobility of large molecules and the water environment were investigated [22–24]. This short overview of the science programme demonstrates that Osiris contributes to a wide and diverse range of challenging problems. To stay at the forefront of scientific discoveries upgrade projects are under way or are proposed.

Here we present an overview of upgrade activities to further expand the capabilities of the Osiris beamline. At present, the energy resolution will be improved with the installation of a silicon analyzer. Within the Endeavour project of the ISIS facility the primary spectrometer will be upgraded with a huge gain in intensity and we are looking further into the future where plans emerge to improve the energy resolution towards μeV.

2 The silicon analyzer project

Opposite to the pyrolytic graphite analyzer side inside the vacuum tank there is an empty space, which will be filled with a silicon analyzer. To enhance the performance of Osiris with respect to energy resolution and allow novel

challenging studies such as slow diffusive motions of ions in battery materials, an upgrade is under way to implement a Si111 analyzer unit with an energy resolution of $\Delta E \approx 11 \ \mu eV$ [25]. On pulsed sources silicon as analyzer material is applied to increase the energy resolution towards μeV [26–28]. In combination with position sensitive detectors the third direction in momentum space can be resolved, which is not possible with the detectors at the existing pyrolytic graphite analyzer. Figure 1 shows a schematic of the parts which will be installed into the vacuum tank. The silicon analyzer crystals are arranged
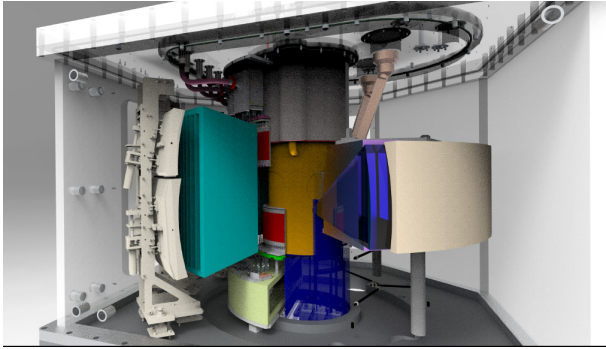
Figure 1. A schematic engineering drawing of the new Si analyzer bench with the two detector arrays and the radial collimator is shown inside the vacuum tank. On the right side of the picture the existing graphite analyzer bench is drawn.

on a radius of 880 mm from the sample axis position and will have a total height of about 700 mm. Hence the total covered solid angle of the secondary spectrometer will be around 2 sr. The silicon analyzer is split into an upper and a lower bench. The neutrons will therefore be reflected into two radial detector arrays, which consist of position sensitive half-inch diameter ^{3}He-detector tubes with a sensitive length of 160 mm (the tubes are colored in red in figure 1). Each analyser bench consists of 4 frames. Two frames are mounted onto a single tower mechanics (grey structure on the left in figure 1). The Bragg angle (about 83°) of the analyzer frames can be aligned through a stepping motor. The preamplifier electronics will be mounted near to the helium tubes and will be housed in an air box (yellow box in figure 1) . Between the analyzer and detectors a coarse radial collimator will be positioned (aqua color in figure 1).

There are several advantages in using silicon compared to pyrolytic graphite. Since Si111 has no second order reflection, there is no need for the installation of a cooled beryllium filter. In addition, due to the lack of thermal diffuse scattering from the analyzer crystals itself no cooling of the whole analyzer bench is needed. However, as-grown silicon wafers are perfect crystals and as such would select a too small wavelength range in comparison with the incoming wavelength band. The reflected wavelength band is given by the Darwin width which corresponds to $\frac{\Delta\lambda}{\lambda} \approx 1.2 \cdot 10^{-5}$ for the Si111 reflection [29].

To overcome the mismatch in resolution between the primary and secondary spectrometer, elastic deforma-

tion of the silicon crystals is applied, which increases the reflected intensity substantially. The deformation is achieved through gluing the wafers onto the spherical frame [30]. The elastic deformation results in a gradient in lattice spacing, Δd, which depends on the curvature radius of the analyzers, R_A, and the thickness of the wafers, D, according to Eq. (1) [30], with $\mu_{eff} \approx 0.4$ being an average Poisson ratio and the small contribution from the Darwin width is omitted.

$$\frac{\Delta d}{d} = \mu_{eff} \frac{D}{R_A} \qquad (1)$$

With a wafer thickness of D=0.8 mm and a radius of R_A=880 mm we might obtain $\frac{\Delta d}{d} = 3.6 \cdot 10^{-4}$, which provides a large increase in reflected intensity.

To reduce background from the aluminium frame the backside of the silicon wafers will be covered by an absorbing layer. Several tests with neutrons have been performed to select the best combination of absorbing material and glue. It became clear that spraying provides a more homogenous coating than adding the paint with a brush. Also, tests with homemade water based resins could be excluded.

Finally, a Gd_2O_3-paint emerged as the best option. Several wafers have been glued onto aluminium disks with a radius of R=880 mm to confirm the viability of the whole process. Figure 2 shows the results of some tests with Si-wafers. One pure Si-wafer, not glued onto a disk, was also measured for comparison reasons. The wafers cut in hexagonal shape had a diameter of about 100 mm. The beam cross section of 20×40 mm^2 only covers the middle part of the wafers. The measurements were made on Osiris using the transmission monitor for transmission measurements and the diffraction detectors for measurements of the reflected background. A few of the 960 available pixels from the diffraction detector were used which are not affected by Bragg reflections and hence monitor the incoherent background from hydrogen scattering. The detector is about 1 m away from the wafers in a backscattering geometry, hence similar to the later application except that no collimator is installed. The reflected signal is used as a measure for the background caused by the glue. A wavelength range around 6.3-8 Å was used. Panel (a) shows the transmitted signal over time-of-flight of the neutrons for a pure Si-wafer (circle) and a Si-wafer (circle) glued on the aluminium disk without an absorbing layer. The transmitted signal is nearly identical and might allow the neutrons to be scattered inelastically in the thick aluminium frame and come back towards the detectors. This would deteriorate the instrument background at least for inelastic spectroscopy. All the other wafers have been covered by absorbing paint, where the *thin layer* wafer (triangle down) shows that a coverage of about 0.8g of absorbing paint per wafer reduces the amount of transmitted neutrons by a factor 30. However, the three *thick layer* wafers (stars) provide a transmission reduction of about a factor 1000. Practically no neutron scattered back from the aluminium frame has a chance to reach the detectors. Typically 2g of absorbing paint has been applied onto these three wafers. In panel (b) of figure 2 the measured re-
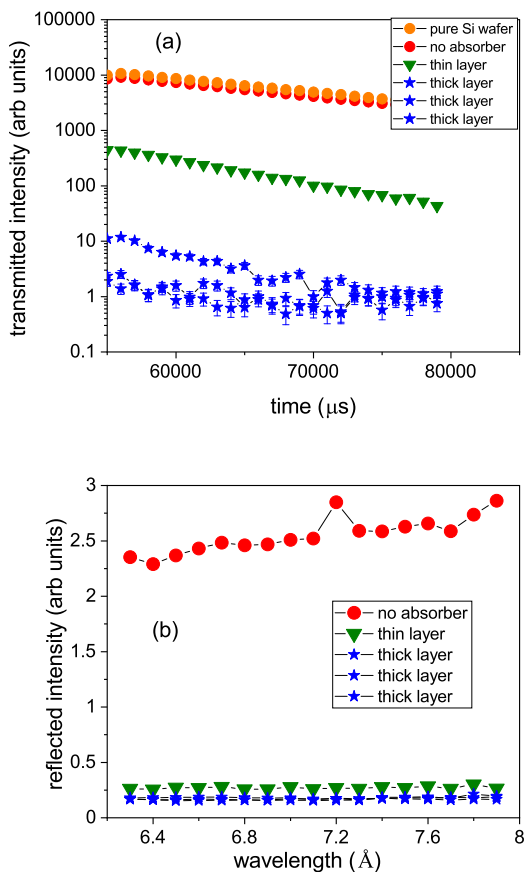
Figure 2. Panel (a) shows transmission measurements on a logarithmic scale against the time-of flight for Si-wafers. In panel (b) the reflected signal from the glued wafers is plotted against the wavelength, which is a measure for incoherent background from the silicon analyzer.

flected background from the wafers is depicted against the wavelength. These results clearly demonstrate that the absorbing layer reduces the overall background by an order of magnitude compared to the glued wafer without an absorbing layer. Note that these measurements were made without a collimator between wafer and detector and hence will be a relative measure for the background with the silicon analyzer. There are practically no differences in reflected background neutrons within the three wafers with thick absorbing layers, which confirm the reliability of the whole process. As a conclusion from all the tests we have chosen an absorbing layer of $\approx 120\ \mu m$ thickness using a commercially available absorbing paint with a 47% Gd_2O_3 content, which is sprayed onto the wafers before they are glued onto the aluminium frame. A square test frame with 300 mm side length has successfully been produced and we are now in the process of building the whole analyzer frame. Installation and commissioning of the Si-analyzer bench is foreseen for 2024.

3 The upgrade of the primary spectrometer

The current Osiris guide is a straight $m = 2$ supermirror guide with a $m = 3.6$ linear focusing section at the end, where m stands for m-times the critical angle of total reflection of a natural-Ni coated guide. The non-negligible number of reflections of long wavelength neutrons in a small cross section guide will reduce the transmission of neutrons decisively. This is the cause for the quite modest gain factor in flux of about 1.6 at $\lambda \approx 6$ Å for Osiris in comparison with the natural Ni guide on the Iris beamline [5].

New guide geometries have less reflections and can transport cold neutrons very effectively over long distances [31, 32]. The performance of these novel guide geometries has been assessed several times in the past (see for example [33–35]) and the elliptic geometry emerged as the most favorable one. Therefore, a new guide with an elliptic defocusing and focusing geometry has been proposed to replace the present Osiris guide [36–38]. The position of the secondary spectrometer will not be moved and to avoid direct line of sight a curved section with a curvature radius of R=1208 m sits between the elliptic sections. Furthermore, the elliptic geometry allows to focus neutrons on a smaller sample size, a necessity when it comes to investigate small sample quantities. Extensive MonteCarlo simulations have been performed to optimize the geometry and coating [36, 38]. The resulting gain factors, defined as the intensity ratio between new and present guide at sample position are shown in figure 3. The simulations predict intensity gain factors between 5 and 7. In addition, a new hydrogen moderator is in process of being installed at target station 1, which is predicted to provide an intensity gain factor of about 2 [39]. All together, one can expect intensity gain factors between 10 and 14 at the sample position, which will enable new experiments, that are nowadays not possible. This intensity increase will keep Osiris competitive with the most modern spectrometers at more powerful sources, albeit not achieving the high energy resolutions offered on these spectrometers [38]. The
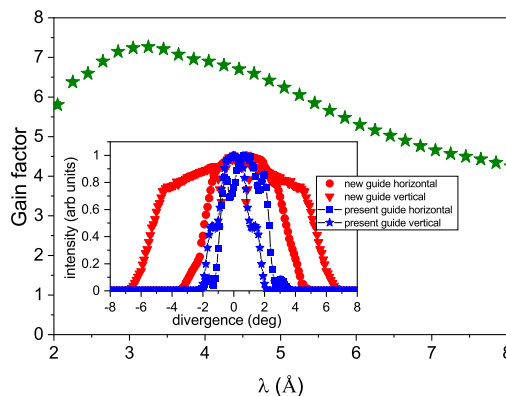
Figure 3. The intensity gain over wavelength is plotted for the new guide. The insert shows the increase in divergence with the new geometry in comparison with the existing guide.

increased flux comes with the prize of an increase in divergence, which is often not detrimental for most of the QENS experiments. The insert in figure 3 shows the vertical and horizontal divergences of the present guide and the new guide. The divergence might increase by up to factor 3 with a more smooth distribution compared to current guide with a linear focusing section. A slit system with 3 movable slits will be integrated into the guide offering a reduction of the divergence by up to a factor 3, which might be necessary when low energy dispersive excitations should be resolved. Of course, the divergence reduction is accompanied by an intensity reduction, because the divergence reduction can be directly related to a reduction in gain. The new guide will have an increased height with a maximum value of 200 mm, which requires to change the bandwidth chopper system. The increased opening and closing times of these slow rotating choppers would reduce the dynamic range of the spectrometer. For this reason a double disc chopper system will be installed with a slightly larger diameter per disc.

4 Towards μeV resolution

To achieve an even higher energy resolution on Osiris one has to consider the main factors to the energy resolution for a tof-backscattering instrument [6, 40]. For the incoming energy it is the pulse width from the moderator, which sets a limit for the energy resolution. To reduce this term one can choose a poisoned moderator and increase the length of the instrument [26] or use a fast pulse shaping chopper [27, 28], which then also provides some flexibility in trading resolution against intensity. With these steps in shortening the pulse width an energy resolution of a few μeV was achieved in a near-backscattering geometry. The main contribution to the final energy uncertainty stems from the Bragg reflection in combination with a divergence term: $\cot(\theta_B)\Delta\theta$ [6]. The divergence term $\Delta\theta$ is dominated by the sample height for a silicon analyzer. The energy resolution term with $\cot(\theta_B)$ will become smaller with increasing Bragg angle towards 90°, but there are technical limitations to be observed. In a near-backscattering geometry the maximum Bragg angle θ_B is dictated by the sample to analyzer distance and the need to install the detectors near the sample position without shadowing the solid angle towards the analyzer bench. Increasing the distance will allow larger Bragg angles, but will limit the solid angle and hence the measured intensity. Geometries with a Bragg angle of 87° and a distance of 2500 mm have been realized and represent the limit [26, 27].

Backscattering spectrometers at reactor sources achieve a higher energy resolution of less than 1 μeV by using a direct backscattering geometry [29, 30, 41]. Consequently, to achieve a lower energy resolution one way forward is to abandon the near-backscattering geometry and apply the direct backscattering geometry at a tof-backscattering spectrometer. For direct backscattering it has been shown that the geometric contribution to the energy resolution is given by [42]:

$$\frac{\Delta E}{E} = 2\{\frac{\Delta\tau}{\tau} + \frac{1}{8}\Delta\theta^2\} \qquad (2)$$

Here $\frac{\Delta\tau}{\tau}$ represents the contribution from the deformation of the lattice constants due to the bending of the wafers, see Eq. 1. The second term is due to the divergence $\Delta\theta$ which is mainly caused by the size of the sample. It is worth mentioning that in the derivation of this equation different contributions to the energy resolution are added directly.

Now we are in a position to calculate the expected energy resolution for the Osiris instrument, using a fast pulse shaping chopper and direct backscattering from the silicon analyser. Assuming a pulse width of $\Delta t = 20\,\mu s$ and a sample height of 30 mm in a distance of 880 mm we calculate the energy resolution for the near-backscattering geometry ($\theta_B = 83^o$) and for the direct backscattering geometry. The results are shown in figure 4. For the near-backscattering geometry we obtain values of $\approx 12\,\mu$eV, which are similar to the values predicted previously for this geometry, except that this value is now achieved for a large sample of 30 mm height. The reduction in energy resolution is due to the pulse shaping chopper although this pulse width shortening will cancel any eventual gain in intensity due to the larger sample. Hence, for this range in energy resolutions the installation of a pulse shaping chopper appears not to be particularly beneficial. Previously we demonstrated that the contribution from the secondary spectrometer for the silicon analyzer near-backscattering geometry of Osiris with a 10 mm large sample has a lower limit of around 6 μeV [25] and is still short of a μeV resolution.

However, when a direct backscattering geometry can be achieved in combination with a fast pulse shaping chopper an energy resolution of $\approx 2\,\mu$eV can be obtained (see figure 4). For this calculation a sample height of 30 mm and a width of 20 mm are assumed.

This upgrade of the Osiris instrument does not need a complete rebuild of the instrument and could be implemented in an evolutionary way. The new 50Hz counter rotating double disc bandwidth choppers could be replaced by similar fast rotating choppers. The installation of the silicon analyzers includes motors for changing the Bragg angle and the mechanics is designed in such a way that the change from near-backscattering to direct backscattering could be done during an experiment without direct intervention inside the vacuum tank. For the direct backscattering geometry a further detector array positioned opposite to the existing detector arrays of the silicon analyzer needs to be installed, which should be movable out of the scattering plane not to block the graphite side when used. Now MonteCarlo simulations are envisaged to assess the performance of this novel setup in detail.

5 Conclusions

Over the past 25 years of operation Osiris was living through a continuous evolution in capabilities. From a cold neutron diffractometer Osiris morphed into a world
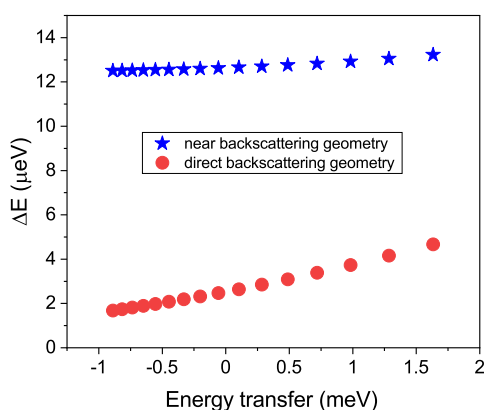
Figure 4. The calculated energy resolution of the Osiris spectrometer is shown for the case using a near-backscattering geometry of the Si analyzer and the resolution when direct backscattering will be employed for a sample with a height of 30 mm. A short pulse of $\Delta t = 20\ \mu s$ is applied through a fast pulse shaping chopper.

leading low-energy spectrometer. This enabled a successful science programme around quantum materials and energy research with high impact publications. There is no standstill and currently the capabilities will be further enhanced through the installation of the silicon analyzer. This upgrade will allow access to longer relaxation times and the survey of full four-dimensional $S(Q, \omega)$ maps of single crystals. The next step will be a decisive increase in intensity with the upgrade of the primary spectrometer. This will assure the competitiveness of Osiris with similar spectrometers at more powerful sources. Further into the future there exists the possibility to extend the resolution capabilities towards μeV. All these improvements will allow Osiris to stay at the forefront of low-energy spectroscopy in the coming decades.

References

[1] D. Martin y Marero, S. Campbell, C.J. Carlile, *J Phys Soc Jpn* **65** 245 (1996)

[2] D. Martin y Marero, D. Engberg, *Physica B* **267-268** 134 (1999)

[3] D. Martin y Marero, *Appl Phys A* **74** Materials Science S289 (2002)

[4] K.H. Andersen, D. Martin y Marero, D. Barlow, *Appl Phys A* **74** Materials Science S237 (2002)

[5] M.T.F. Telling and K.H. Andersen, *Phys Chem Chem Phys* **7** 1255 (2005); M.T.F. Telling, S.I. Campbell, D. Engberg, D. Martin y Marero, K.H. Andersen, *Phys Chem Chem Phys* **18** 8243 (2016)

[6] F. Demmel and K. Pokhilchuk, *Nucl Instr Meth A* **767** 426 (2014)

[7] F. Demmel D. McPhail, C. French, D. Maxwell, S. Harrison, J. Boxall, N. Rhodes, S. Mukhopadhyay, I. Silverwood, V. Garcia Sakai, F. Fernandez-Alonso, *J Phys Conf Ser* **1021** 012027 (2018)

[8] F. Demmel, D. McPhail, J. Crawford, D. Maxwell, K. Pokhilchuk, V. Garcia-Sakai, S. Mukhopadyay, M.T.F. Telling, F.J. Bermejo, N.T. Skipper, F. Fernandez-Alonso, *EPJ Web of Conferences* **83** 03003 (2015)

[9] R. Coldea, D.A. Tennant, E.M. Wheeler, E. Wawrzynska, D. Prabhakaran, M. Telling, K. Habicht, P. Smeibidl, K. Kiefer, *Science* **327** 177 (2010).

[10] C. Stock, C. Broholm, Y. Zhao, F. Demmel, H.J. Kang, K.C. Rule, C. Petrovic, *Phys Rev Lett* **109** 167207 (2012)

[11] C. Stock, E.E. Rodriguez, N. Lee, M.A. Green, F. Demmel, R.A. Ewings, P. Fouquet, M. Laver, Ch. Niedermayer, Y. Su, K. Nemkovski, J.A. Rodriguez-Rivera, S.-W. Cheong, *Phys Rev Lett* **117** 017201 (2016)

[12] W.J. Gannon, I.A. Zaliznyak, L.S. Wu, A.E. Feiguin, A.M. Tsvelik, F. Demmel, Y. Qiu, J.R.D. Copley, M.S. Kim, M.C. Aronson, *Nat Comm* **10** 1123 (2019)

[13] G.S. MacGlashan, Y.G. Andreev, P.G. Bruce, *Nature* **398** 792 (1999)

[14] T.J. Willis, D.G. Porter, D. J. Voneshen, S. Uthayakumar, F. Demmel, M.J. Gutmann, M. Roger, K. Refson, J. P. Goff, *Scientific Reports* **8** 3210 (2018)

[15] M.K. Gupta,S. K. Mishra, R. Mittal, B. Singh, P. Goel, S. Mukhopadhyay, R. Shukla, S.N. Achary, A. K. Tyagi, S.L. Chaplot, *Phys Rev Mat* **4** 045802 (2020)

[16] R. Laven, U. Häussermann, A. Perrichon, M. S. Andersson, M. Sannemo Targama, F. Demmel, M. Karlsson, *Chem Mater* **33** 2967 (2021)

[17] G.J. Irvine, F. Demmel, H.Y. Playford, G. Carins, M.O. Jones, J.T.S. Irvine, *Chem Mater* **34** 9934 (2022)

[18] A.M.A. Leguy, J. Moore Frost, A.P. McMahon, V. Garcia Sakai, W. Kockelmann, C. Law, X. Li, F. Foglia, A. Walsh, B.C. O Regan, J. Nelson, J.T. Cabral, P.R.F. Barnes, *Nat Comm* **6** 7124 (2015)

[19] B. E. Meijer, G. Cai, F. Demmel, H.C. Walker, A.E. Phillips, *Phys Rev B* **106** 064302 (2022)

[20] A.J. O Malley, V. Garcia Sakai, N. Dimitratos, W. Jones, C.R.A. Catlow, S.F. Parker, *Phil. Trans. R. Soc. A* **378** 20200063 (2020); A.J. OMalley, S.F. Parker, C.R.A. Catlow, *Chem Comm* **53** 12164 (2017)

[21] S.K. Matam, C.R.A. Catlow, I.P. Silverwood, A.J. OMalley, *Topics in Catalysis* **64** 699 (2021)

[22] V. Arrighi, J. Tanchawanich, M.T.F. Telling, *Macromolecules* **46** 216 (2013)

[23] M. P. M. Marques, A.L.M. Batista de Carvalho, V. Garcia Sakai, L. Hatter, L.A.E. Batista de Carvalho, *Phys Chem Chem Phys* **19** 2702 (2017)

[24] F. Foglia, A.J. Clancy, J. Berry-Gair, K. Lisowska, M.C. Wilding, T.M. Suter, T.S. Miller, K. Smith, F. Demmel, M. Appel, V. Garcia-Sakai, A. Sella, C. A. Howard, M. Tyagi, F. Cora, P.F. McMillan, *Sci Adv* **6** eabb6011 (2020)

[25] A. Perrichon, F. Fernandez-Alonso, M. Wolff, M. Karlsson, F. Demmel, *Nucl Instr Meth A* **947** 162740 (2019)

[26] E. Mamontov and K.W. Herwig, Rev Sci Instrum **82** 085109 (2011)

[27] N. Takahashi, K. Shibata, T.J. Sato, Y. Kawakita, I. Tsukushi, N. Metoki, K. Nakajima, M. Arai *Nucl Instr Meth A* **600** 91 (2009); K. Shibata, N. Takahashi, Y. Kawakita, M. Matsuura, T. Yamada, T. Tominaga, W. Kambara, M. Kobayashi, Y. Inamura, T. Nakatani, K. Nakajima, M. Arai, *Jap Phys Soc Conf Proc* **8** 036022 (2015)

[28] N. Tsapatsaris, R.E. Lechner, M. Markó, H.N. Bordallo, *Rev Sci Instrum* **87** 085118 (2016); N. Tsapatsaris, P.K. Willendrup, R.E. Lechner, H.N. Bordallo, *EPJ Web of Conferences* **83** 03015 (2015)

[29] B. Frick, E. Mamontov, L. van Eijck, T. Seydel, *Zeit Phys Chem* **224** 33 (2010)

[30] A. Meyer, R.M. Dimeo, P.M. Gehring, D.A. Neumann, *Rev Sci Instrum* **74** 2759 (2003)

[31] C. Schanzer, P. Böni, U. Filges, T. Hils, *Nucl Instr Meth A* **529** 63 (2004)

[32] K.H. Kleno, K. Lieutenant, K.H. Andersen, K. Lefmann *Nucl Instr Meth A* **696** 75 (2012)

[33] H. Jacobsen, K. Lieutenant, C. Zendler, K. Lefmann *Nucl Instr Meth A* **717** 69 (2013)

[34] C. Zendler, D. Nekrassov, K. Lieutenant, *Nucl Instr Meth A* **746** 39 (2014)

[35] D.M. Rodriguez, D.D. DiJulio, P.M. Bentley, *Nucl Instr Meth A* **808** 101 (2016)

[36] A. Perrichon, F. Fernandez-Alonso, M. Wolff, M. Karlsson, F. Demmel, *Journal of Surface Investigation: X-ray, Synchrotron and Neutron Techniques* **14** S169 (2020)

[37] A. Perrichon, and F. Demmel, *Technical Report TR RAL* 002 (2020)

[38] A. Perrichon and F. Demmel, *Nucl Instr Meth A* **1039** 167014 (2022)

[39] G. Skoro, S. Lilley, R. Bewley, *Physica B* **551** 381 (2018)

[40] F. Demmel and K. H. Andersen, *Meas Sci and Tech* **19** 034021 (2008)

[41] J. Wuttke, A. Budwig, M. Drochner, H. Kämmerling, F.-J. Kayser, H. Kleines, V. Ossovyi, L.C. Pardo, M. Prager, D. Richter, G.J. Schneider, H. Schneider, S. Staringer, *Rev Sci Instrum* **83** 075109 (2012)

[42] M. Birr, A. Heidemann, B. Alefeld, *Nucl Instr Meth A* **95** 435 (1971)